JACS
JOURNAL OF THE AMERICAN CHEMICAL SOCIETY

ARTICLE

pubs.acs.org/JACS

Lipid Binding to the Carotenoid Binding Site in Photosynthetic Reaction Centers

Sasmit S. Deshmukh, Kai Tang, and László Kálmán*

Department of Physics, Concordia University, Montreal, Quebec H4B 1R6, Canada

Supporting Information

ABSTRACT: Lipid binding to the carotenoid binding site near the inactive bacteriochlorophyll monomer was probed in the reaction centers of carotenoid-less mutant, R-26 from *Rhodobacter sphaeroides*. Recently, a marked light-induced change of the local dielectric constant in the vicinity of the inactive bacteriochlorophyll monomer was reported in wild type that was attributed to structural changes that ultimately lengthened the lifetime of the charge-separated state by 3 orders of magnitude (Deshmukh, S. S.; Williams, J. C.; Allen, J. P.; Kalman, L. *Biochemistry* **2011**, *50*, 340). Here in the R-26 reaction centers, the combination of light-induced structural changes and lipid binding resulted in a 5 orders of magnitude increase in the lifetime of the charge-separated state involving the oxidized dimer and the reduced primary quinone in proteoliposomes. Only saturated phospholipids with fatty acid chains of 12 and 14 carbon atoms long were bound successfully at 8 °C by cooling the reaction center protein slowly from room temperature. In addition to reporting a dramatic increase of the lifetime of the charge-separated state at physiologically relevant temperatures, this study reveals a novel lipid binding site in photosynthetic reaction center. These results shed light on a new potential application of the reaction center in energy storage as a light-driven biocapacitor since the charges separated by ~30 Å in a low-dielectric medium can be prevented from recombination for hours.

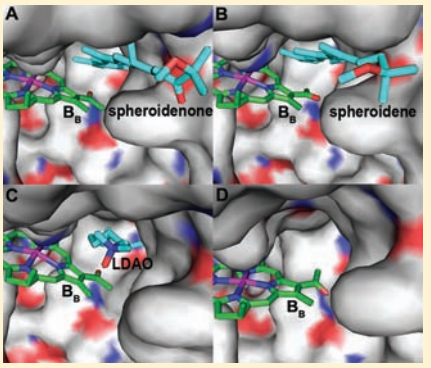

INTRODUCTION

Nature's photosynthetic apparatus offers at least three different model examples for solar energy conversion that can inspire humanity to develop artificial light-driven energy converters for future energy production and storage: (i) catalytic splitting of water in oxygenic photosynthetic organisms, (ii) generation of proton-electrochemical gradient in both oxygenic and anoxygenic systems, and (iii) creation of long-lived, energetic charge-separated states in many photosynthetic enzymes. Both water splitting and the formation of a transmembrane proton gradient require the co-operation of at least two membrane-bound enzymes and the accumulation of multiple electron equivalents.[1,2] Generation of a long-lived charge-separated state, on the other hand, can be achieved by a single enzyme with the transfer of only one electron. The reaction center (RC) from purple photosynthetic bacteria has been used widely as a structural and functional model for examining the general principles of biological electron transfer for decades.[3] It has also played an important role in the design and construction of artificial photosynthetic complexes.[4,5] The RC from *Rhodobacter sphaeroides* has three polypeptides, L, M, and H, of which the L and M subunits bind two branches (A and B) of cofactors arranged in a pseudo-2-fold symmetry that runs perpendicular to the plane of the membrane.[6] Despite this symmetry, electron transfer takes place only along the A-branch. The wild-type (WT) RC also incorporates a tightly bound carotenoid molecule in the close vicinity of the inactive bacteriochlorophyll monomer (B_B) that is responsible for photoprotection of the RC (Figure 1). This binding site was successfully reconstituted earlier with various carotenoids, and as demonstrated in Figure 1, detergent molecules, such as *N*-lauryl-*N*,*N*-dimethylamine N-oxide (LDAO) or octyl β-glucoside (BOG) were also reported to bind to this site in the carotenoid-less mutant, R-26.[7−9] Light initiates a transfer of an electron from a dimer of two bacteriochlorophyll molecules (P), via one of the monomeric bacteriochlorophyll (B_A) and bacteriopheophytin (H_A) to the primary quinone (Q_A) and if available to the secondary quinone (Q_B), leading to a charge separation across the photosynthetic membrane.[2] The lifetimes of the single flash-induced $P^+Q_A^-$ and $P^+Q_B^-$ charge-separated states, in agreement with the Marcus theory, were found as 0.1 and 1 s, respectively.[3,10] While this range of lifetimes is sufficiently long enough to allow the utilization of the stored energy by the organism, it is too short to be considered useful for man-made energy storage. It has been shown for various processes that the observed rate can substantially be altered if the electron transfer is coupled to and limited by another process, such as proton transfer or conformational change.[11−13] In a recent series of work,[14−16] we have demonstrated that the lifetime of the $P^+Q_A^-$ charge pair can be increased from 100 ms to 16 min by the combination of systematic alteration of the environment of the charges and light-induced structural changes near P in RCs from both *Rba. sphaeroides* and *Rhodobacter capsulatus*. In the present study we

Received: August 16, 2011
Published: September 06, 2011

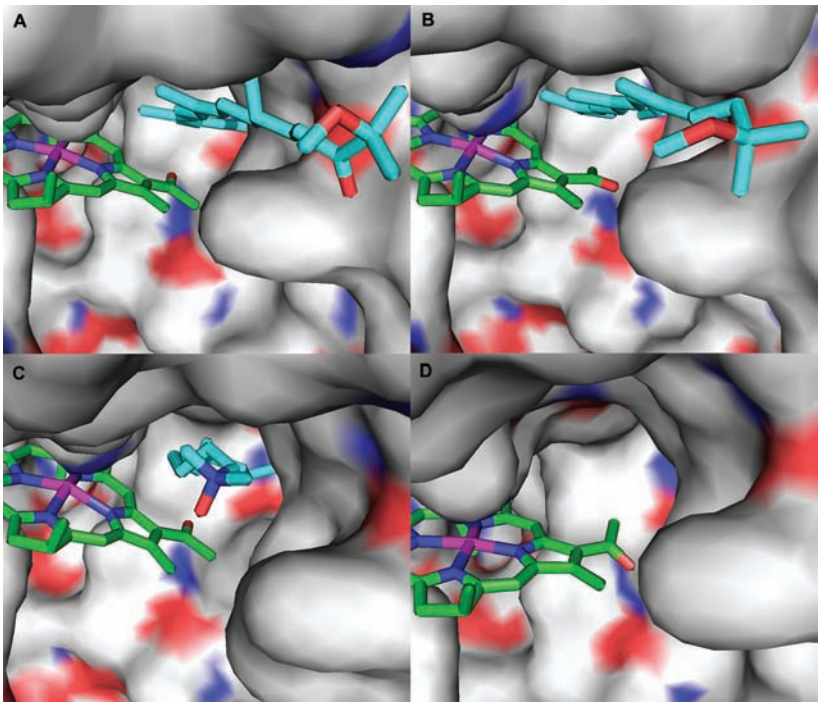

Figure 1. Surface representation of the carotenoid binding site near B_B as viewed from the entrance of the cavity that has access to the surrounding. Negatively charged regions are indicated with red, positively charged ones with blue, and neutral areas with gray. The B_B molecule is color-coded by its atoms: carbon (green), nitrogen (blue), oxygen (red), and the central Mg^{2+} (magenta). The hydrophobic chains of the bound molecules are indicated with light blue. The site is shown occupied by a spheroidenone (A), a spheroidene (B), and an LDAO (C), molecule. The empty pocket is also shown (D). Coordinates were taken from the following PDB entry codes for each panel: (A) 2GMR, (B) 1PCR, (C) 1RG5, and (D) 1OGV.

combine lipid binding to the carotenoid binding site near B_B and replacement of the detergent micelles with liposomes to increase the lifetime of the $P^+Q_A^-$ state even further to hours in the R-26 strain. Although the RC is arguably the most studied integral membrane protein, very little is known about how individual lipid molecules influence the function of the protein. Recent high-resolution X-ray structures identified three integral lipid molecules, but a definite functional role could not be assigned to them unambiguously.[17,18] These lipids were modeled in earlier structures as detergent molecules. Even less is known about the functional role of B_B in the carotenoid-less R-26 as it was removed successfully by a sodium borohydrate treatment without altering the rapid electron-transfer rates, such as charge separation, cytochrome oxidation, and charge recombination.[19] In this work we report the effects of lipid binding near B_B on the light-induced structural changes, and we discuss the role of B_B in the lipid binding and charge stabilization.

MATERIALS AND METHODS

Bacterial Growth and RC Isolation. Cells from WT *Rba. sphaeroides* were grown both anaerobically under light and semiaerobically in the dark to incorporate a spheroidene or a spheroidenone molecule in the carotenoid binding site, respectively. The carotenoid-less mutant, R-26 was also grown under these conditions. The RCs were isolated and purified by use of *N*-lauryl-*N*,*N*-dimethylamine N-oxide (LDAO) according to methods described earlier.[13−15] The purity of the RCs, defined as the ratio of absorbance at 280 and 802 nm, was below 1.6 for all preparations. For some experiments the LDAO detergent was replaced with the neutral detergent Triton X-100 (TX-100) by ion-exchange chromatography. Due to the repetitive chromatography steps, the secondary quinone activity was only ∼10% as checked by flash-induced absorption changes measured with a miniaturized laser flash photolysis unit (LFP-112 from Luzchem Research Co., Ottawa, Ontario, Canada). Routinely 100 μM terbutryn was used in all preparations to eliminate any secondary quinone activity. Reconstitution of the RCs to unilamellar vesicles was performed by the gel-filtration, micelle-to-vesicle transition method as described in detail in our recent work.[16] The following lipids were used: 1,2-dilauroyl-*sn*-glycero-3-phosphocholine (DLPC), 1,2-dimyristoyl-*sn*-glycero-3-phosphocholine (DMPC), and 1,2-dioleoyl-*sn*-glycero-3-phosphocholine (DOPC). All lipids were purchased from Avanti Polar Lipids (Alabaster, AL) and were used without further purification. Addition of the lipids to detergent-dispersed RCs was performed according to Nagy et al.[20] to maintain both the ∼1000:1 lipid/protein ratio and the 0.05% TX-100 concentration. All RC purification and handling steps were done in near darkness to ensure that the samples remained strictly in the dark-adapted states before the controlled illuminations during the recording of spectra and kinetics. All measurements were performed at pH 7.

Optical Spectroscopy. Optical spectra and kinetics of the absorbance changes induced by continuous illumination were measured with a Varian Cary 5000 spectrophotometer equipped with a Peltier cell cooled temperature control unit (Mulgrave, Victoria, Australia). Illumination was performed according to methods described recently.[14−16] The spectra were recorded at the maximum ∼1800 nm/min scanning rate. Kinetic traces were analyzed by decomposition into exponentials via the Marquardt nonlinear least-squares method. All measurements were performed in the 6−30 °C temperature range.

RESULTS

Influence of Added Lipids on Lifetime of the $P^+Q_A^-$ State after Prolonged Illumination. RCs from anaerobically grown WT and R-26 strains dispersed in TX-100 detergent micelles were illuminated in the presence and absence of various lipids, and the kinetics of absorption changes after prolonged, subsaturating illumination was monitored at the center of the P-band at 865 nm at pH 7. Figure 2 shows these recovery kinetic traces recorded at two different temperatures: 22 °C (panel A) and 8 °C (panel B). The illumination time was selected at both temperatures to meet the following criteria: (i) saturation of the signals in all samples before the illumination was terminated, (ii) fully recovering absorption changes at 865 nm, and (iii) maximizing the lifetime of the charge-separated state. The complex recovery kinetics after the illumination indicates that long-lived, conformationally altered forms of the $P^+Q_A^-$ charge pair were formed in fractions of the RCs besides the unresolved (in the minute scale) transient changes as reported earlier by many studies.[13−16,21−23] At 22 °C, the overall recovery kinetics was faster in the R-26 (trace a) than in WT (trace e), and the fraction of RCs that underwent light-induced structural changes was also smaller in R-26 than in WT. A similar observation was made for semiaerobically grown WT and R-26 (Figure S1 in Supporting Information). Rate constants and relative amplitudes for the slower kinetic components for the anaerobically grown samples are tabulated in Table S1 (Supporting Information). In R-26 only the component with a rate constant of $\sim 10^{-2}$ s^{-1} was detected, while in WT an additional, slower component with a rate constant of $\sim 10^{-3}$ s^{-1} was also observed in a small fraction of RCs. These long-lived kinetic components were identified in our recent studies conducted in RCs from semiaerobically grown WT from *Rba. sphaeroides* and *Rba. capsulatus* as arising from conformational changes near P.[14−16] The chosen lipids all had the same zwitterionic phosphocholine (PC) headgroup with zero net charge at the selected pH to avoid electrostatic perturbations in the RCs. The length of the fatty acid chain and the saturation level was altered by using dilauroyl (12 carbon atoms long chain with zero double bonds, C12:0), dimyristoyl (C14:0), and dioleoyl (C18:1) chains in DLPC, DMPC, and DOPC, respectively. Addition of lipids at 22 °C had only a minor effect on the kinetics in R-26, except for DMPC, and had practically no effect at all in WT (Figure 2A). In the presence of DMPC (trace c), a slight increase of the lifetime was observed. At 8 °C the difference between the recovery kinetics in R-26 (trace a) and in WT (trace e) became even more pronounced and the influence of the lipids altered the lifetime of the charge pair very differently in R-26. The presence of DOPC (trace b) did not induce any change but both DMPC (trace c) and DLPC (trace d) increased the lifetime of the $P^+Q_A^-$ state. The effect was especially pronounced for DLPC where the recovery kinetics became unexpectedly longer in R-26 than in WT with rate constants of 7.0×10^{-4} s^{-1} and 1.1×10^{-3} s^{-1} for the slowest components in R-26+DLPC and in WT, respectively. It must be noted that the pronounced effect of the saturated lipids were observed only if the samples were cooled with a slow, 0.2 °C/min rate. Unlike in R-26 the addition of DLPC did not induce any further change in the lifetimes for WT regardless of the cooling rate (trace f).

Spectral Signatures Associated with Bound Carotenoid and Lipid. Room-temperature light-minus-dark optical difference spectra of dark-adapted RCs from WT and R-26 dispersed in TX-100 are expected to be similar in the near-infrared

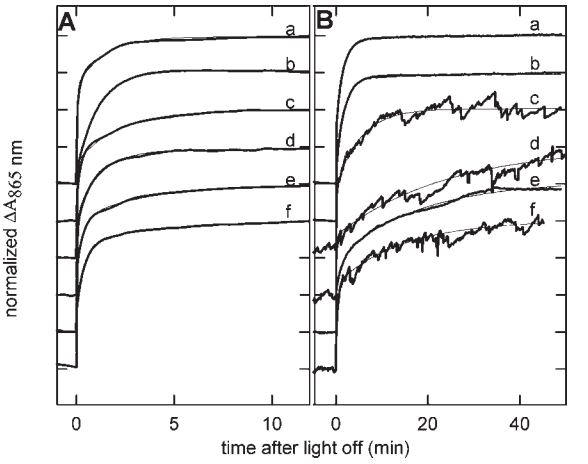

Figure 2. Kinetics of light-induced absorption changes at (A) 22 °C and (B) 8 °C, measured at the center of the Q_y absorption band of P after the illumination was turned off. The following samples were used: (a) R-26, (b) R-26 + DOPC, (c) R-26 + DMPC, (d) R-26 + DLPC, (e) WT, and (f) WT + DLPC. The illumination time was 5 and 20 min for panels A and B, respectively. The traces were normalized to the maximum absorbance changes at time = 0 and were shifted vertically for clarity. Thin solid lines are the best fits to the curves. The results of the fits are tabulated in Table S1 (Supporting Information). Conditions: 1 μM RCs, 15 mM Bis-tris-propane, pH 7.0, 1 mM EDTA, and 0.05% TX-100.

spectral region, as major differences are observed only in the 450−600 nm range due to absorption of the carotenoid in WT.[24] Spectra recorded in the presence of terbutryn at pH 7 in RCs from both strains feature the absorption decrease of the Q_y band of P centered at ∼865 nm; an electrochromic blue shift of the B-band around 800 nm, due to the interaction between the positively charged P^+ and the accessory bacteriochlorophylls (B_A and B_B); and an electrochromic red shift of the H-band due to interaction between Q_A^- and the two H molecules.[25] Figure 3 shows these absorption changes recorded in anaerobically grown WT and R-26 (panels A and B) and in R-26 in the presence of DLPC lipid at 22 °C (panel C) and at 8 °C (panel D). Comparison of the presented spectra recorded immediately after the illumination started (solid lines) reveals that the extent of electrochromic absorption change of the B-band is considerably larger in WT (panel A), which binds a carotenoid molecule near B_B, than in the carotenoid-less R-26 (panel B). A similar trend can be observed in RCs from semiaerobically grown cells (Figure S2, Supporting Information). Although the presence of DLPC at room temperature did not alter the light-induced spectra of R-26 (panel C) at 8 °C, the extent of electrochromic absorption change of the B-band has increased significantly (panel D). Figure 3 also shows the normalized spectra recorded immediately after the prolonged illumination was turned off (dashed lines). While the spectra recorded at the beginning of the illumination are characteristic to dark-adapted RCs those collected after the prolonged illumination can be attributed to RCs that underwent light-induced structural changes.[14] The decrease of electrochromic absorption change of the B-band during the prolonged illumination was also much smaller in R-26 than in WT, as indicated by the double difference spectra (thick solid lines). The extent of prolonged illumination-induced electrochromic absorption changes of the B_B band was found recently to be a sensitive probe of the local electric field and of the light-induced structural changes near P in RCs from both *Rba.*

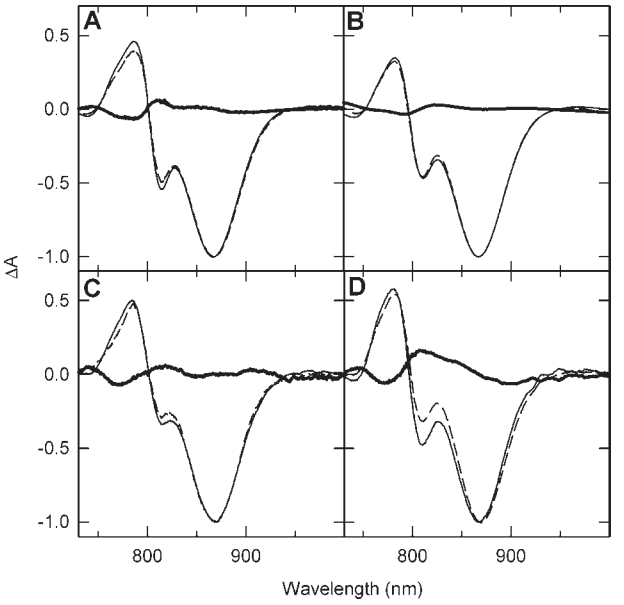

Figure 3. Normalized light-minus-dark difference spectra, recorded (—) immediately after the onset of the light and (---) 1 min after the illumination was turned off, for RCs isolated from anaerobically grown cells: (A) WT; (B) R-26; and R-26 + DLPC at (C) 22 °C (C) and (D) 8 °C. The thick solid lines show the double difference spectra (dashed-minus-solid) and feature changes around 800 nm consistent with the decrease of electrochromic absorption changes involving the monomers during the illumination. Conditions were as described for Figure 2.

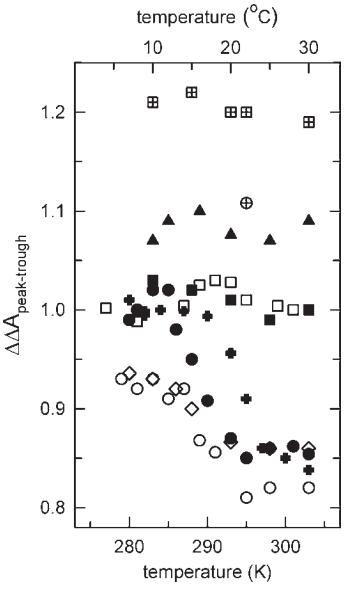

Figure 4. Temperature dependence of the peak-to-trough amplitude of the electrochromic absorption changes around 800 nm for RCs isolated from anaerobically grown cells: (□) WT, (■) WT + DLPC, (○) R-26, (◇) R-26 + DOPC, (+) R-26 + DMPC, (●) R-26 + DLPC, and (▲) R-26 in 1% LDAO. For comparison, the same parameters in WT (⊞) and R-26 (⊕) from semiaerobic growth are also shown. The data were taken from light-minus-dark difference absorption spectra recorded immediately after the onset of illumination and normalized to the maximum of the P band. The error of the measurements is ±0.02 absorbance unit. Conditions were as described for Figure 1 except for (▲), where 0.05% TX-100 was replaced with 1% LDAO.

sphaeroides and *Rba. capsulatus*.[14,16] Corresponding to the smaller light-induced spectral changes in R-26, the amplitude of the long-lived $P^+Q_A^-$ state in the recovery kinetics recorded at 865 nm was also smaller in the carotenoid-less mutant without added lipids (see Figure 2A, traces a and e, and Figure S1 and Table S1 in Supporting Information). In the presence of DLPC at room temperature, the prolonged illumination-induced decrease remained small but at 8 °C this decrease of the electrochromic absorption change of the B-band became very large.

Since the peak-to-trough amplitude of the electrochromic absorption change was sensitive to the presence or absence of the hydrophobic carotenoid molecule, growth conditions, and added lipids, this parameter was measured as a function of temperature in the 6−30 °C range in RCs mostly dispersed in TX-100. Moreover, this spectral feature was found recently to be correlated with the local dielectric constant near B_B.[14] As shown in Figure 4, the amplitude of this absorption change was large and was found, within error, to be independent of the temperature in both anaerobically and semiaerobically grown WT and in anaerobically grown R-26 dispersed in relatively high (1%) concentrations of LDAO. In general, the electrochromic absorption changes in RCs from semiaerobically grown cells were larger than those found in RCs from anaerobically grown cells for both WT and R-26 in TX-100 (see Figure 3 and Figure S2 in Supporting Information). The presence of added DLPC did not change this value in WT. LDAO was specifically selected because an LDAO molecule was reported earlier to occupy the carotenoid binding site in R-26 for samples dispersed in LDAO detergent micelles (Figure 1C). In the presence of added DLPC and DMPC, the extent of electrochromic absorption change showed pronounced temperature dependence in anaerobically grown R-26. As the temperature was lowered, the initially small spectral changes in the 24−18 and 20−12 °C temperature ranges increased and then leveled off at lower temperatures in the presence of DMPC and DLPC, respectively. Interestingly, with decreasing temperature a slight increase was also observed in the anaerobically grown R-26 even without added lipids, and DOPC also caused only moderate temperature dependence. The absorption changes in the presence of the saturated lipids were sensitive to the cooling rate as stated above.

Influence of Liposomes on Light-Induced Conformational Changes. Figure 5 shows the kinetics of recovery of the $P^+Q_A^-$ charge pair at 22 °C (panel A) and 8 °C (panel B) in RCs from anaerobically grown WT and R-26 that have been incorporated into liposomes formed from various lipids with different hydrophobic thicknesses and saturation levels. The kinetic traces were generated by plotting the absorption changes at 868 nm taken from the spectra recorded at different times during and after the illumination, as demonstrated for three data points in Figure 5B. Rate constants and relative amplitudes of the kinetic components in the recovery kinetics are tabulated in Table S2 (Supporting Information). At 22 °C, the lifetime of the $P^+Q_A^-$ state in R-26 was found to be 2.5-fold longer in liposomes from DOPC, which has a long fatty acid chain (C18), than in liposomes from DLPC with a shorter (C12) chain. When RCs from WT with the hydrophobic spheroidene molecule near B_B were incorporated into the same DLPC liposomes, the lifetime was nearly a factor of 2 longer than in R-26. The relative amplitude of this long-lived component was also larger in WT than in R-26, in agreement with the observations made in detergent-dispersed RCs (Figure 2 and Figure S1 in Supporting Information). This relationship became radically different at 8 °C, where the lifetimes were extremely long

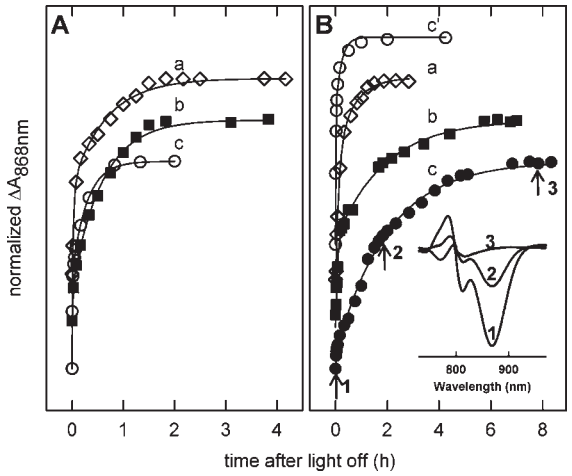

Figure 5. Kinetics of the light-induced absorption changes at (A) 22 °C and (B) 8 °C, measured at the center of the Q_y absorption band of P after the illumination was turned off in RCs reconstituted into liposomes from various lipids. The following samples were used: (a, ◇) R-26 in DOPC, (b, ■) WT in DLPC, (c, ○, ●) R-26 in DLPC, and (c′, ○) R-26 in DLPC with rapid cooling. The traces were normalized to the maximum absorption changes at time = 0 and were shifted vertically for clarity. Thin solid lines are the best fits to the curves. The results of the fits are tabulated in Table S2 (Supporting Information). Conditions: ∼1.5 μM RCs, 15 mM phosphate (mono- and disodium) buffer, pH 7, 15 mM KCl, 100 μM terbutryn.

(∼2 h) in DLPC liposomes for both WT (trace b) and R-26 (trace c), with rate constants of 1.5×10^{-4} s^{-1} and 1.3×10^{-4} s^{-1}, respectively. Moreover, the fraction of the component with this ultralong lifetime reached 93% in R-26 as compared to 58% in WT. As seen from the inset in Figure 5B, the electrochromic absorption changes of the B-band were still observable even after complete recovery of the $P^+Q_A^-$ charge pair 8 h after the illumination was turned off (trace c). This very long lifetime, however, could be achieved only if the RCs were cooled at a slow rate of 0.2 °C/min. Rapid cooling (4 °C/min rate) of RCs from R-26 in DLPC liposomes resulted in exactly an order of magnitude faster recovery with a rate constant of 1.3×10^{-3} s^{-1} and in only 36% of the RCs (trace c′). The same temperature decrease in DOPC liposomes caused the lifetime of the charge-separated state to change only by ∼1.4-fold in R-26 RCs. Unlike in DLPC, the cooling rate had no influence of the recovery kinetics in DOPC liposomes.

■ DISCUSSION

The binding of various lipids with different fatty acid chain lengths and saturation levels to the carotenoid binding site near B_B was probed in RCs from the carotenoid-less R-26 mutant both in micelles and in liposomes. The influence of the added lipids on the stability of the long-lived $P^+Q_A^-$ charge pair was very different and temperature-dependent for the saturated lipids, indicating an important role of the phase behavior of the lipids. In a recent series of studies, we have presented evidence that light-induced structural changes near P are responsible for the long lifetime of the charge-separated state after prolonged illumination in both *Rba. sphaeroides* and *Rba. capsulatus*.[14−16] A correlation between the structural changes and several properties, including significant decrease of the P/P^+ potential, electrochromic absorption change of the band of the nearby B_B molecule due to the change in local dielectric constant, and proton release from the periplasmic side, was established. In this work, these studies on carotenoid-containing RCs have been extended to the RCs from the carotenoid-less R-26 strain, which shows pronounced spectral and kinetic differences in comparison with WT in the presence and absence of lipids. The results suggest a temperature-dependent binding of DLPC and DMPC lipids to R-26 but not to WT RCs.

Dependence of Binding on Phase Behavior of the Lipid. Comparison of the recovery kinetics of WT and R-26 RCs dispersed in detergent micelles suggests that the presence of the bound carotenoid molecule in WT provides a larger degree of stabilization than the empty binding site in R-26 for the $P^+Q_A^-$ charge pair in the light-adapted conformation (Figure 2 and Figure S1 in Supporting Information). Of the three lipids used in this study, addition of DMPC to R-26 RCs increased the lifetime of the charge-separated state at both 22 and 8 °C; DLPC had the greatest influence but only at 8 °C; and DOPC did not provide any stabilization at either temperature (Figure 2). As none of the lipids induced any change in either the spectra or kinetics in WT, our results are consistent with binding of the lipids to the carotenoid binding site in their ordered but not in their disordered phase. In the liquid crystalline phase the acyl chains are disordered, requiring more space than in the ordered phase, where the chains become parallel and fully extended. The phase transition temperature of pure DMPC determined by light scattering measurements was reported as 24.7 °C, and he presence of the RC with a 4000:1 lipid:RC ratio in liposomes caused it to shift to 27 ± 2 °C.[26,27] The same parameters for DLPC are 0 and 11 ± 3 °C, respectively.[27] In the presence of the RC protein, the phase transition curves of these lipids were also reported to be broadened by 2.5−4 °C compared to the phase transition behavior of pure lipids. Due to these factors, the complete phase transition in the presence of the RC protein was reported to occur at ∼28−25 °C and at ∼17−7 °C for DMPC and DLPC, respectively.[26] These reported ranges are in reasonable agreement with the temperature dependences of the electrochromic absorption changes of the B-bands that exhibited a pronounced increase in the ∼24−18 °C range for DMPC and ∼20−10 °C range for DLPC in mixed micelles (Figure 4). Besides the two main phases an intermediate phase, the ripple phase, was also observed in various saturated phospholipids upon phase transition.[28,29] The structure of the ripple phase for DLPC was found to be heavily dependent upon the cooling rate.[30] Slow cooling with rates between 0.1 and 1 °C/min favored the formation of a long ripple phase with higher degree of hydration than the short ripple phase obtained with rapid cooling. The lateral diffusion coefficients were reported to be dependent upon the hydration level with nearly 2 orders of magnitude slower values in the gel phase than in the liquid-crystalline phase.[31] The faster diffusion reported earlier in DLPC than in DMPC supports the longer lifetime caused by the presence of DLPC in this study (Figure 2).[32] The absence of any influence of DOPC on the recovery kinetics in the detergent-solubilized RCs is consistent with the lack of binding of this lipid, as the phase transition temperature of DOPC (−20 °C) is well below the investigated temperature range. The lack of DOPC binding is also supported by the same temperature dependence of the electrochromic absorption change in the presence and absence of DOPC in R-26 (Figure 4). Moreover, the carotenoid binding site was modeled empty in the crystal structure of R-26 determined from the lipidic cubic phase where the membrane around the RCs was composed of lipids with monooleyl (C18:1) chains, similar to

that found in DOPC (Figure 1D).[33] In R-26 at 8 °C in DLPC liposomes, the lifetime of the longest-lived charge-separated state was more than 5-fold longer than in TX-100 micelles mixed with DLPC (Figures 2 and 5; Tables S1 and S2, Supporting Information). Additionally, the amplitude of the longest-lived component rose from 60% in detergent to 93% in liposomes. Thus, it is obvious that binding of DLPC to the carotenoid binding site alone cannot account for the very long lifetime of the charge-separated state measured at 8 °C in DLPC liposomes. It has been shown recently that the lifetime of the $P^+Q_A^-$ state at room temperature in the light-induced conformation could be increased by 2-fold if the RCs from *Rba. capsulatus* were incorporated into DOPC liposomes, where the lipid bilayer thickness was matched by the hydrophobic thickness of the RC, but not in DLPC liposomes, with shorter than desired bilayer thickness.[16] As at 22 °C, neither DOPC nor DLPC is expected to bind to the carotenoid binding site; the nearly 2.5-fold longer lifetime in DOPC liposomes for R-26 is consistent with this earlier finding (Figure 5A and Table S2, Supporting Information). A similar 2-fold difference in the rate constants could still be observed at 8 °C if the DLPC liposomes were cooled rapidly, suggesting that rapid cooling in DLPC liposomes prevents the binding of the lipid due to the dramatically decreased diffusion rate of the lipid as discussed above (Figure 5B). In the gel phase the thickness of the DLPC bilayer was reported to be 27.0 Å, as opposed to 19.5 Å in the liquid crystalline phase, indicating that at 8 °C the DLPC bilayer may provide a reasonable hydrophobic thickness for the transmembrane α-helices of the RCs with a thickness of ~30 Å.[34,35]

Carotenoid Binding Pocket. The bound carotenoid in WT is located ~11 Å from P, and it is in van der Waals contact with B_B.[36] Its closeness to both B_B and P justifies the pronounced differences in both kinetics (Figure 2 and Figure S1 in Supporting Information) and spectra (Figure 3 and Figure S2 in Supporting Information) between WT and R-26. B_B also has the single largest surface area contribution in the binding pocket.[7] Besides B_B, the pocket is composed of 29 mostly hydrophobic amino acids. Both the natural and the reconstituted carotenoids bind to the same position, adopting the 15−15′-cis configuration. The carotenoids used for reconstitution, however, were in all-trans isomeric configuration upon addition, indicating that the isomerization must take place upon binding.[7] The molecules to be bound to the pocket should enter only from the entrance shown in Figure 1 with tail-in-first orientation since the other end was reported to be blocked by Phe M162, which serves as a gatekeeper.[7] The binding pocket is quite flexible, as significant differences in the tunnel shape and diameter were reported in the presence and absence of the carotenoid.[7] The much shorter LDAO molecule, with its chain length of 12 carbons, was reported to occupy the central portion of the pocket only 3.6 Å away from the acetyl group of B_B.

Orientation of the Acetyl Group of B_B. A correlation between the orientation of the 2-acetyl group of B_B and the extent of the electrochromic absorption changes can be established by comparing structural details with our results presented in Figure 4. Structural studies based on X-ray crystallography modeled the orientation of the acetyl group of B_B differently, depending on the occupation of the carotenoid binding site (Figure 1, Table 1). In all cases the acetyl group was assumed to be more or less in the plane of the tetrapyrrole macrocycle and thus, part of the conjugation. This is in agreement with earlier spectroscopic studies and our present results that detected no

Table 1. List of PDB Codes for Representative Structures That Show Orientation of the Acetyl Group of B_B Depending on the Molecule Occupying the Carotenoid Binding Site

bound molecule near B_B	θ^a	PDB code	ref
	WT		
spheroidenone	in	2GMR	37
spheroidenone	in	2BOZ	38
spheroidenone	in	1UMX	39
spheroidenone	in	1K6L	40
spheroidenone	in	3DSY	unpublished
spheroidene	out	1RVJ	43
spheroidene	out	1PCR	41
spheroidene	out	1YST	35
spheroidene	out	1KBY	18
spheroidene	out	2J8C, 2UWS	42
	R-26		
3,4-dihydrospheroidene	in	1RQK	7
spheroidene	in	1RGN	7
LDAO	in	2HG3, 2HG9	8
LDAO	in	1RG5	7
none	out	1OGV	33

[a] θ is the orientation of oxygen atom of the acetyl group of B_B viewed from the entrance of the binding pocket.

significant blue shift in the absorption band of B_B in the absolute optical spectra (Figure 3 and Figure S2 in Supporting Information). When the site was occupied with a spheroidenone molecule in RCs from semiaerobically grown WT (Figure 1A), the oxygen atom of the acetyl group was modeled facing inward.[37−40] If, however, the site was occupied with spheroidene in WT (Figure 1 B) from anaerobic growth, the oxygen of the acetyl group was modeled facing outward.[35,41,42] Corresponding to these orientations, the electrochromic absorption changes in the semiaerobically grown WT were significantly larger than in WT from anaerobically grown cells. In both cases these changes were temperature-independent, suggesting that the rotation of the acetyl group is not favored if a carotenoid molecule occupies the binding site (Figure 4 and Figure S2 in Supporting Information). It must be noted that the inward orientation was proposed in all cases when the binding site was reconstituted in the carotenoid-less R-26 mutant with spheroidene or 3,4-dihydrospheroidene or when an LDAO molecule (Figure 1 C, Table 1) was modeled to occupy this site.[7] In contrast, the opposite orientation was found when the binding site was empty (Figure 1D) in R-26 when the crystals were grown from a lipidic cubic phase.[33] The different levels measured for electrochromic absorption changes in TX-100 and in the presence of 1% LDAO for R-26 are consistent with the proposed rotation of the acetyl group from "out" to "in" upon binding of LDAO. Our results in LDAO also suggest that the acetyl group should be oriented inward in the semiaerobically grown R-26. Since the electrochromic absorption changes are inversely proportional to the local dielectric constant around the interacting P and B_B molecules, these changes in WT are expected to be larger than in R-26 due to the presence of a hydrophobic carotenoid molecule in the immediate vicinity of B_B in WT (Figure 3 and Figure S2 in Supporting Information). Our results also support the rotation of the acetyl group from the "out" to the "in" orientation in the

20−15 °C range as the temperature is lowered in the anaerobically grown R-26 (Figure 4). This rotation appears to be required for the binding of a lipid molecule, as in the presence of DLPC and DMPC the electrochromic absorption changes followed similar temperature dependence, although with larger differences between the two extremes. The slight differences in this temperature dependence for DLPC and DMPC are most likely due to the different *in situ* phase transition temperatures of the lipids as discussed earlier. The inward orientation for lipid binding is also supported by crystallographic studies that modeled this conformation for any bound molecules other than the naturally synthesized spheroidene (Table 1).[7,8,35,41,42] Even though the correlation appears to be strong, it should also be mentioned that in moderate-resolution crystal structures (>2 Å), such as those available for the RCs from *Rba. sphaeroides*, it could be challenging to determine the orientation of the acetyl group directly from the electron density. Since the expected electron density difference between the "in" and "out" orientations is very small, the best bet is usually based on identification of potential hydrogen-bonding partners for the carbonyl oxygen. Unfortunately, for B_B a potential hydrogen-bond donor is absent in most of the cases. Therefore the proposed orientation may suffer from bias by the molecular replacement starting model or automatic choice of chemical restraints, where one torsion angle is favored over the other. For example, in the case of the special pair, where His L168 and Tyr M210 were suggested to be hydrogen-bond donors for the carbonyl oxygen atoms, in some models the carbonyl oxygen is modeled pointing away from the potential hydrogen-bond donor.[43,44] In our recent studies we proposed Tyr M210 to be hydrogen-bonded to the acetyl group of P_B but only in the light-induced conformation.[14,15] This indicates that the experimental conditions, in particular the dark adaptation of the RCs, may have significant influence on this structural detail.

Implications of Results for Protein Function and Potential Applications. Despite of the symmetrical arrangement of the pigment cofactors along two branches in the RCs, only one branch was functionally active in the charge-separation process. Extensive studies have led to the current view that suggests an energetic asymmetry between the two branches due to different interactions of the cofactors with their surroundings along the two branches.[45,46] Recent improvements in crystallographic studies identified three tightly bound lipids in the RCs that were modeled in earlier structures as detergent molecules.[17,18] A glycolipid molecule was found near the active bacteriochlorophyll monomer (B_A), which most likely shields this cofactor from the external solvent and provides a hydrophobic environment.[18] As the electron from P to H_A is transferred via B_A, the low dielectric constant is optimal for setting a low reorganization energy for this electron-transfer step.[3] Contrarily, the inactive bacteriochlorophyll monomer (B_B) has no bound lipid and was found to have access to the polar solvent.[19] Many structures modeled a detergent molecule to accommodate the electron density found in the carotenoid binding pocket in R-26. One might speculate whether a lipid molecule can occupy this binding site in R-26, similarly to the other three lipids that were modeled also as detergents in earlier structures. Although binding of a lipid molecule near B_B to the carotenoid-binding site in R-26 may influence the probability of charge separation along the inactive branch, other factors must also contribute to the unidirectional electron transfer, as the rate of charge separation was essentially the same in R-26 and WT regardless of the presence of a bound carotenoid molecule in WT. For example, the presence of another integral lipid, the phosphocholine near only H_B, should also contribute to the functional asymmetry.[18] Our results indicated that at any given illumination conditions the RCs from R-26 mutant have lower ability to undergo structural changes than WT RCs. The structural changes were reported recently to reduce the P/P^+ potential and thus lower the risk of oxidative damage if, due to excess light, the RC becomes saturated and the cytochrome c_2 and/or quinone pools become exhausted.[15] In the photosynthetic membranes, the RCs from WT are surrounded by light-harvesting complexes 1 and 2 (LH1 and LH2). The amount of LH2 is synchronized with the available light, and changes in the ambient light exposure can adjust the LH2 level. The LH2 complex, however, was removed from R-26, hindering its ability to adjust for changes for the light conditions. It seems reasonable to develop a compensating mechanism for the removed two lines of defense (lack of LH2 and carotenoid) in R-26 involving lipid binding that can increase the probability of light-induced structural changes that can lower the potential of the P/P^+ couple. Although the RCs and many other membrane proteins are typically studied in a detergent environment, the integral lipids that gained cofactor status recently should also interact with the membrane lipids, which supply *in vivo* an environment with functional properties radically different from those of the isolated protein. These interactions allowed the charge-separated state to last for an unprecedented long time.

Expansion of the lifetime of the charge-separated state from 100 ms to hours at a convenient temperature range presented in this work provides a new opportunity to utilize the RC as a light-driven biocapacitor in energy storage. The principles leading to the ability of the RC to store electric potential on an extended time scale can be inspiring for the development of biomimetic systems that can form the basis of molecular-scale optoelectronic devices.

Abbreviations. RC, reaction center; P, bacteriochlorophyll dimer; B_A and B_B, bacteriochlorophyll monomers in the A and B branch, respectively; H_A and H_B, bacteriopheophytin molecules in the A and B branch, respectively; Q_A, primary quinone; Q_B, secondary quinone; *Rba.*, *Rhodobacter*; WT, wild type; TX-100, Triton X-100; LDAO, *N*-lauryl-*N*,*N*-dimethylamine N-oxide; BOG, octyl β-glucoside; DOPC, 1,2-dioleoyl-*sn*-glycero-3-phosphocholine; DLPC, 1,2-dilauroyl-*sn*-glycero-3-phosphocholine; DMPC, 1,2-dimyristoyl-*sn*-glycero-3-phosphocholine; C*N*:*X*, fatty acid chains with *N* carbon atoms and *X* double bonds; LH1 and LH2, light harvesting complexes 1 and 2, respectively.

■ ASSOCIATED CONTENT

Supporting Information. Two figures, showing kinetics of absorption changes and light-minus-dark optical difference spectra for RCs from semiaerobically grown WT and R-26, and two tables, listing rate constants determined in micelles and proteoliposomes. This material is available free of charge via the Internet at http://pubs.acs.org.

■ AUTHOR INFORMATION

Corresponding Author
laszlo.kalman@concordia.ca

■ ACKNOWLEDGMENT

This work was supported by a grant from Natural Sciences and Engineering Research Council of Canada.

REFERENCES

(1) *Oxygenic Photosynthesis: The Light Reactions*; Ort, D. R., Yocum, C. F., Eds.; Kluwer Academic Publishers: Dordrecht, The Netherlands, 1996.

(2) *The Purple Phototropic Bacteria*; Hunter, C. N., Daldal, F., Thurnauer, M. C., Beatty, J. T., Eds.; Springer Verlag: Dordrecht, The Netherlands, 2008.

(3) Marcus, R. A.; Sutin, N. *Biochim. Biophys. Acta* **1985**, *811*, 265.

(4) Gust, D.; Moore, T. A.; Moore, A. L. *Acc. Chem. Res.* **2001**, *34*, 40.

(5) Hammarström, L.; Sun, L. C.; Akermark, B.; Styring, S. *Spectrochim. Acta, Part A* **2001**, *57*, 2145.

(6) Allen, J. P.; Feher, G.; Yeates, T. O.; Komiya, H.; Rees, D. C. *Proc. Natl. Acad. Sci. U.S.A.* **1987**, *84*, 5730.

(7) Roszak, A. W.; McKendrick, K.; Gardiner, A. T.; Mitchell, I. A.; Isaacs, N. W.; Cogdell, R. J.; Hashimoto, H.; Frank, H. A. *Structure* **2004**, *12*, 765.

(8) Roszak, A. W.; Gardiner, A. T.; Isaacs, N. W.; Cogdell, R. J. *Biochemistry* **2007**, *46*, 2909.

(9) Yeates, T. O.; Komiya, H.; Chirino, A.; Rees, D. C.; Allen, J. P.; Feher, G. *Proc. Natl. Acad. Sci. U.S.A.* **1988**, *85*, 7993.

(10) Moser, C. C.; Keske, J. M.; Warncke, K.; Farid, R. S.; Dutton, P. L. *Nature* **1992**, *355*, 796.

(11) Graige, M. S.; Paddock, M. L.; Bruce, J. M.; Feher, G.; Okamura, M. Y. *J. Am. Chem. Soc.* **1996**, *118*, 9005.

(12) Tiede, D. M.; Vázquez, J.; Córdova, J.; Marone, P. *Biochemistry* **1996**, *35*, 10763.

(13) Kálmán, L.; Maróti, P. *Biochemistry* **1997**, *36*, 15269.

(14) Deshmukh, S. S.; Williams, J. C.; Allen, J. P.; Kálmán, L. *Biochemistry* **2011**, *50*, 340.

(15) Deshmukh, S. S; Williams, J. C.; Allen, J. P.; Kálmán, L. *Biochemistry* **2011**, *50*, 3321.

(16) Deshmukh, S. S.; Akhavein, H.; Williams, J. C.; Allen, J. P.; Kálmán, L. *Biochemistry* **2011**, *50*, 5249.

(17) McAuley, K. E.; Feyfe, P. K.; Ridge, J. P.; Isaacs, N. W.; Cogdell, R. J.; Jones, M. R. *Proc. Natl. Acad. Sci. U.S.A.* **1999**, *96*, 14706.

(18) Camara-Artigas, A.; Brune, D.; Allen, J. P. *Proc. Natl. Acad. Sci. U.S.A.* **2002**, *99*, 11055.

(19) Maróti, P.; Kirmaier, C.; Wraight, C.; Holten, D.; Pearlstein, R. M. *Biochim. Biophys. Acta* **1985**, *810*, 132.

(20) Nagy, L.; Milano, F.; Dorogi, M.; Agostiano, A.; Laczkó, G.; Szebényi, K.; Váró, G.; Trotta, M.; Maróti, P. *Biochemistry* **2004**, *43*, 12913.

(21) Goushcha, A. O.; Kharkyanen, V. N.; Holzwarth, A. R. *J. Phys. Chem. B* **1997**, *101*, 259.

(22) Andréasson, U.; Andréasson, L. E. *Photosynth. Res.* **2003**, *75*, 223.

(23) van Mourik, F.; Reus, M.; Holzwarth, A. R. *Biochim. Biophys. Acta* **2001**, *1504*, 311.

(24) Cogdell, R. J.; Celis, S.; Celis, H.; Crofts, A. R. *FEBS Lett.* **1977**, *80*, 190.

(25) Clayton, R. K. *Photosynthesis: Physical mechanisms and chemical patterns*; Cambridge University Press: Cambridge, U.K., and New York, 1980.

(26) Riegler, J.; Möhwald, H. *Biophys. J.* **1986**, *49*, 1111.

(27) Sperotto, M. M.; Mouritsen, O. G. *Eur. Biophys. J.* **1988**, *16*, 1.

(28) Rappolt, M.; Rapp, G. *Eur. Biophys. J.* **1996**, *24*, 381.

(29) Sun, W.-J.; Tristram-Nagle, S.; Suter, R. M.; Nagle, J. F. *Proc. Natl. Acad. Sci. U.S.A.* **1996**, *93*, 7008.

(30) Dahbi, L.; Arbel-Haddad, M.; Lesieur, P.; Bourgaux, C.; Ollivon, M. *Chem. Phys. Lipids* **2006**, *139*, 43.

(31) Ratto, T. V; Longo, M. L. *Biophys. J.* **2002**, *83*, 3380.

(32) Vaz, W. L. C.; Goodsaid-Zalduondo, F.; Jacobson, K. *FEBS Lett.* **1984**, *174*, 199.

(33) Katona, G.; Andréasson, U; Landau, E. M.; Andréasson, L. E.; Neutze, R. *J. Mol. Biol.* **2003**, *331*, 681.

(34) Dumas, F.; Lebrun, M. C.; Tocanne, J. F. *FEBS Lett.* **1999**, *458*, 271.

(35) Arnoux, B.; Gaucher, J. F.; Ducruix, A.; Reiss-Husson, F. *Acta Crystallogr., Sect. D: Biol. Crystallogr.* **1995**, *51*, 368.

(36) McAuley, K. E.; Fyfe, P. K.; Ridge, J. P.; Cogdell, R. J.; Isaacs, N. W.; Jones, M. R. *Biochemistry* **2000**, *39*, 15032.

(37) Hermes, S.; Stachnik, J. M.; Onidas, D.; Remy, A.; Hofmann, E.; Gerwert, K. *Biochemistry* **2006**, *45*, 13741.

(38) Potter, J. A.; Fyfe, P. K.; Frolov, D.; Wakeham, M. C.; van Grondelle, R.; Robert, B.; Jones, M. R. *J. Biol. Chem.* **2005**, *280*, 27155.

(39) Fyfe, P. K.; Isaacs, N. W.; Cogdell, R. J.; Jones, M. R. *Biochim. Biophys. Acta* **2004**, *1608*, 11.

(40) Pokkuluri, P. R.; Laible, P. D.; Deng, Y. L.; Wong, T. N.; Hanson, D. K.; Schiffer, M. *Biochemistry* **2002**, *41*, 5998.

(41) Ermler, U.; Fritzsch, G.; Buchanan, S. K.; Michel, H. *Structure* **1994**, *2*, 925.

(42) Koepke, J.; Krammer, E. M.; Klingen, A. R.; Sebban, P.; Ullmann, G. M.; Fritzsch, G. *J. Mol. Biol.* **2007**, *371*, 396.

(43) Xu, Q.; Axelrod, H. L.; Abresch, E. C.; Paddock, M. L.; Okamura, M. Y.; Feher, G. *Structure* **2004**, *12*, 703.

(44) Hermes, S.; Stachnik, J. M.; Onidas, D.; Remy, A.; Hofmann, E.; Gerwert, K. *Biochemistry* **2006**, *45*, 13741.

(45) Heller, B. A.; Holten, D.; Kirmaier, C. *Science* **1995**, *269*, 940.

(46) van Brederode, M. E.; van Mourik, F.; van Stokkum, I. H. M.; Jones, M. R.; van Grondelle, R. *Proc. Natl. Acad. Sci. U.S.A.* **1999**, *96*, 2054.